24th IMEKO TC4 International Symposium
22nd International Workshop on ADC and DAC Modelling and Testing
IMEKO TC-4 2020
Palermo, Italy, September 14-16, 2020

A coaxial cryogenic probe for quantum Hall effect measurements in the AC regime

Martina Marzano[1], Ngoc Thanh Mai Tran[1,2], Vincenzo D'Elia[1], Danilo Serazio[1], Emanuele Enrico[1], Massimo Ortolano[2,1], Klaus Pierz[3], Jan Kučera[4], Luca Callegaro[1]

[1]*INRIM Istituto Nazionale di Ricerca Metrologica, Strada delle Cacce 91, 10135, Turin, Italy*

[2]*Politecnico di Torino, Corso Duca degli Abruzzi 24, 10129, Turin, Italy*

[3]*PTB Physikalisch-Technische Bundesanstalt, Bundesallee 100, 38116 Braunschweig, Germany*

[4]*CMI Czech Metrology Institute, Okružní 31, 638 00 Brno, Czech Republic*

***Abstract* – The quantum Hall effect is the basis for the realisation of the resistance and impedance units in the revised International System of units of 2019. This paper describes a cryogenic probe that allows to set graphene Hall devices in quantisation conditions in a helium bath (4.2 K) and magnetic fields up to 6 T, to perform precision measurements in the ac regime with impedance bridges. The probe has a full coaxial wiring, isolated from the probe structure, and holds the device in a TO-8 socket. First characterisation experiments are reported on a GaAs device which shows quantisation at 5.5 T.**

I. INTRODUCTION

In the revised International System of Units (SI) the units of electrical impedance (ohm, henry, farad) can be realised from the quantised Hall resistance $R_\mathrm{H} = R_\mathrm{K}/i$, where $R_\mathrm{K} = h/e^2 = 25\,812.807\,45\ldots\Omega$, the von Klitzing constant, is an exact value [1, Appendix 2] and i is a small integer (typically, $i = 2$). The aim of the project *GIQS: Graphene Impedance Quantum Standard* (see Acknowledgments) is to develop and make available an affordable and easy-to-operate impedance standard exploiting the quantum Hall effect (QHE) in graphene.

Graphene devices are of strong interest for the realisation of electrical units since they display the QHE at lower magnetic fields (below 5 T) and higher temperatures (several K) than semiconductor devices, such the well-established GaAs ones [2, 3, 4, 5]. Hence, the operating conditions can be attained with simpler and less expensive cryogenic systems. However, the direct measurement of the quantised resistance in the ac regime requires careful considerations about device wiring and shielding, to minimise the effects of stray parameters which can alter the apparent resistance of the device from the quantised value [6].

To date, the direct traceability of capacitance to the QHE has been implemented with a coaxial transformer quadrature bridge, using two independent QHE devices in a twin

Fig. 1. A computer rendering of the cryomagnetic probe assembly: (left) side view; (right) front view, showing the magnet bore.

probe [7, 8, 9]. The development of high-accuracy digital impedance bridges [10, 11, 12] opens the possibility for simplified implementations. The GIQS project is pursuing implementations based on a four terminal-pair, fully-digital impedance bridge and a single QHE device, operating in a simple cryogenic environment under relaxed experimental conditions of temperature and magnetic field with respect to common QHE experiments. The target uncertainty is of a few parts in 10^7.

The following describes the realisation of a cryogenic environment for QHE devices, which includes a coaxial cryogenic probe and a superconducting magnet of small size. The environment is suitable to perform QHE experiments at the liquid helium temperature of $4.2\,\mathrm{K}$, and magnetic inductions up to $6\,\mathrm{T}$, hence adequate for graphene QHE devices.

The probe is suitable to be employed with a new fully-digital coaxial impedance bridge [12]. The bridge is optimised to perform RC comparisons with a $1:1$ magnitude ratio, with a comparison uncertainty in the 10^{-7} range. In combination with the probe, it will allow the calibration of a capacitance standard in terms of R_H and therefore the realisation of the unit of capacitance, the farad.

A first test of the probe was performed in the dc regime, using a novel GaAs sample which showing quantization plateaus at reduced magnetic induction ($5.6\,\mathrm{T}$ for the $i = 2$ plateau) with respect to typical devices employed in metrology [6]. The results of the measurement are herewith reported.

II. THE PROBE

A simplified diagram of the probe assembly[1] is shown in Fig. 1. The small size of the probe allows the insertion in a standard dewar having a $50\,\mathrm{mm}$ port, such as transport dewars.

A. *Superconducting magnet*

The probe supports a superconducting magnet (see Fig. 2) that can reach a maximum field of $\pm 6\,\mathrm{T}$ at $4.2\,\mathrm{K}$ when energized with a dc current of approximately $65\,\mathrm{A}$. The field homogeneity is $0.1\,\%$ over a $10\,\mathrm{mm}$ length. The magnet includes a superconducting thermal switch, which allows operation in persistent mode.

B. *Probe insert*

The probe holds a sliding insert. The bottom side of the insert (Fig. 3), which enters the magnet bore, mounts a TO-8 socket connected with 9 coaxial wires[2]. Of these

[1] The probe frame was realised by Graphensic AB, Sweden, according to INRIM specifications.

[2] Lakeshore Ultra Miniature Coaxial Cable, type SC, teflon insulation. The wire has an outer diamter of $1\,\mathrm{mm}$; the inner conductor has a series resistance of $0.282\,\Omega\,\mathrm{mm}^{-1}$ at room temperature; the inner to outer capacitance is $154\,\mathrm{pF\,m}^{-1}$ per unit length.

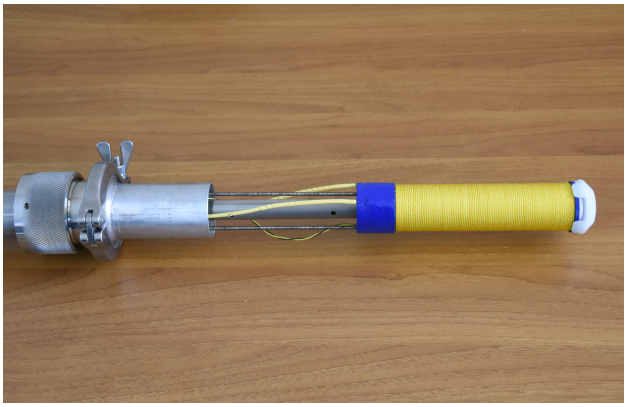

Fig. 2. The probe cryomagnet, showing the yellow winding insulation. A header (white) has been added to ease the insertion in the cryostat.

Fig. 3. The bottom side of the insert, which slides into the cryomagnet bore. The brass shield (right) has been removed, to show the TO-8 socket, which hosts a GaAs device on its TO-8 holder, and the 9 coaxial electrical lines.

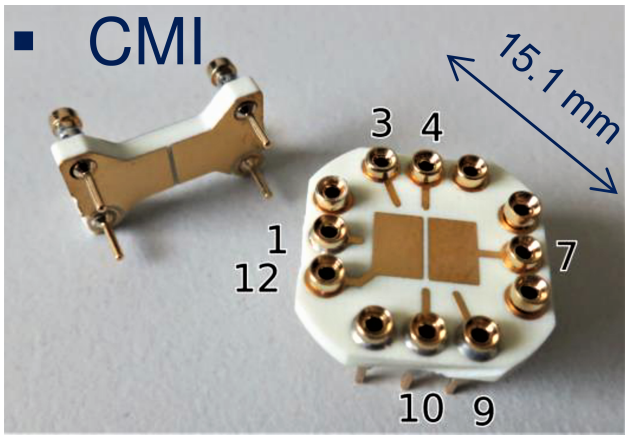

Fig. 4. TO-8 fully coaxial sample holders, implementing the double-shielding technique [13]. After the bonding of the quantum Hall device onto the holder (right), the shielding cap (left) is slid into the socket.

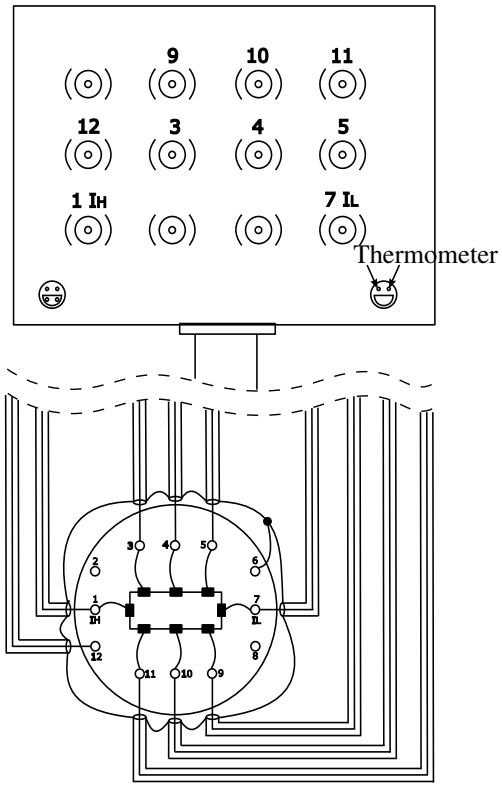

Fig. 5. Schematic diagram of the coaxial connections of the probe. 9 coaxial connections are available, fully isolated from the probe metal bulk. The outer conductors of each line are joined together on the sample holder (pin 6).

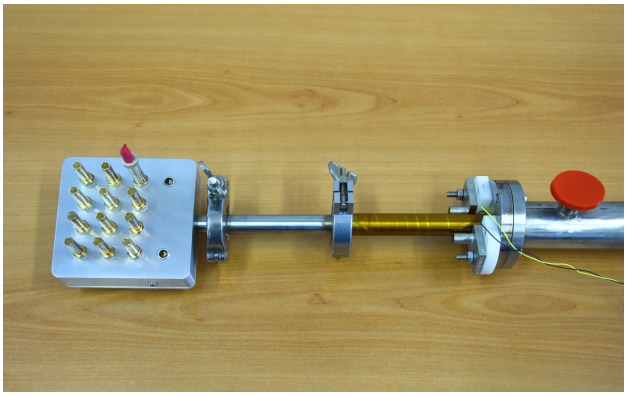

Fig. 6. The probe connection box.

9 wires, 8 are intended to be used on the current and voltage terminals of the device; the 9th wire is available for driving a section of the double shield [13]. Samples can be mounted on special TO-8 sample holders (Fig. 4) implementing a double-shielding technique [13] that minimises the frequency dependence of the quantised Hall resistance caused by unwanted stray capacitances. The outer conductors of the wiring are connected to a common node close to the sample holder.

The coaxial wiring (Fig. 5) is terminated on a connection box at the top of the insert (Fig. 6) with isolated British Post Office Multiple Unit Steerable Array (BPO MUSA) coaxial connectors, typically employed in primary ac impedance bridges. The connectors have a good performance also in the dc regime. The whole coaxial network composed by the device and the wiring is thus isolated from the probe.

C. Operation

Fig. 7 shows the probe in operation. It is inserted into a liquid helium dewar. The magnet is energised with a dc high-current power supply (Cryogenics PS 120A). A manual current-reversing switch allows to reverse the magnetic field polarity.

The superconducting switch in parallel with the magnet is driven by a dc laboratory power supply, which is turned off to activate the persistent mode of operation. The persistent mode maximises field stability and minimizes helium consumption, since the magnet wires are unloaded, and can be used when performing precision measurements on a QHE plateau.

III. TESTING

A test of the probe was made by performing measurement in the dc regime on a GaAs sample. The specific device investigated is P151-24, an AlGaAs/GaAs heterostructure; the growth conditions, sample preparation and metrological characterisation (performed on a similar

Fig. 7. Overall view of the measurement setup for DC characterisation. On the left, the liquid helium dewar, with the coaxial probe inserted. On the right, the rack of electronic instrumentation.

device from the same wafer) are reported in [14]. The device is mounted on an unshielded TO-8 holder with soldered Pt wires.

The device is driven by a purpose-built, isolated and battery operated dc current source. The source can be manually operated to to deliver the current values $I = 0\,\mu\text{A}$, $\pm 5\,\mu\text{A}$, $\pm 20\,\mu\text{A}$, $\pm 50\,\mu\text{A}$ and $\pm 100\,\mu\text{A}$ and includes a fast protection circuit in case of device thermal runaway. The dc voltage on selected contacts is measured with a two-channel nanovoltmeter (Agilent 34420A).

Fig. 8 reports the outcome of the experiment. Fig. 8(a) is the graph of the Hall resistance $R_{\text{H}}(B)$ versus the applied magnetic field B, measured with a current $I = 20\,\mu\text{A}$. Fig. 8(b) shows the corresponding longitudinal resistance $R_{\text{xx}}(B)$. Curves obtained with increasing and decreasing B are shown; a little hysteresis, related to the sweep rate (about $0.6\,\text{T}\,\text{min}^{-1}$) can be appreciated. Increasing the current up to $I = 50\,\mu\text{A}$ gives similar results (not reported).

In Fig. 8(a) quantum Hall plateaux corresponding to filling factors $i = 2$ and $i = 4$ can be easily identified, and also higher-index plateaux can be appreciated. Fig. 8(b) shows the corresponding Shubnikov-de Haas oscillations. On the $i = 2$ plateau, R_{H} is flat over a range of about $0.2\,\text{T}$; the corresponding R_{xx} is lower than $50\,\text{m}\Omega$. The outcome of the experiment is consistent with the expectations on a GaAs device.

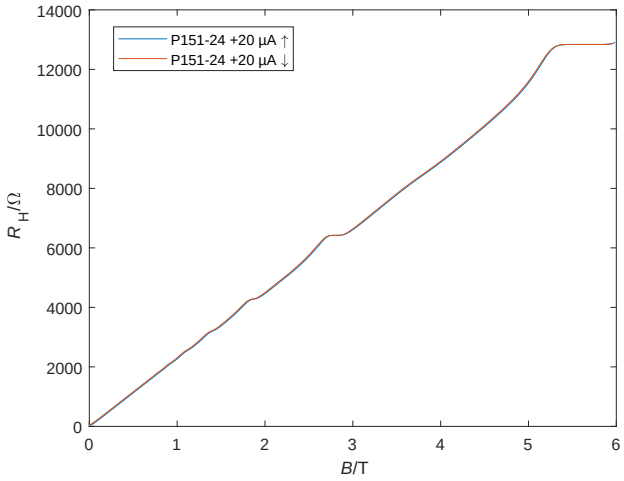

(a) $R_{\text{H}}(B)$

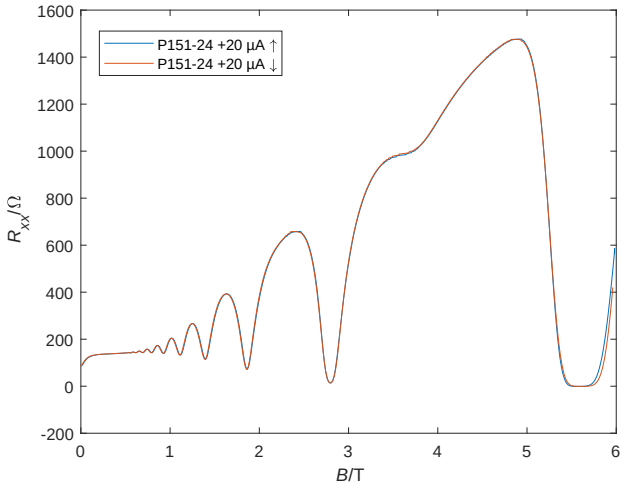

(b) $R_{\text{xx}}(B)$

Fig. 8. Plot of the measured values of R_{H} and R_{xx} versus the magnetic field B, for an applied current $I = 20\,\mu\text{A}$. Blue line: increasing magnetic field. Red line: decreasing magnetic field.

IV. CONCLUSIONS

The test shows that the probe can be employed to reach the quantization condition in Hall devices, and sensitive dc measurements can be performed.

The probe is ready to be employed with a fully-digital coaxial impedance bridge designed for the calibration of a capacitance standard in terms of R_{H} with an uncertainty of a few parts in 10^7. In combination with the probe, the bridge is therefore suitable for the realisation of the unit of capacitance, the farad. The effects of stray parameters will be minimized by exploiting the multiple connections technique [15].

The probe is intended to be used with graphene individual devices and arrays [16], to be developed in the frame of the GIQS project. In the meantime, the GaAs device here investigated will allow to perform first tests of the bridge in operating conditions.

V. ACKNOWLEDGMENTS

GIQS: Graphene Impedance Quantum Standard is a Joint Research Project, code 18SIB07, of the European Metrology Programme for Innovation and Research (EMPIR). This project received funding from the European Metrology Programme for Innovation and Research (EMPIR) co-financed by the Participating States and from the European Union's Horizon 2020 research and innovation programme. Regular updates about the project are posted on the project webpage, `ptb.de/empir2019/giqs` and a LinkedIn group, `linkedin.com/groups/8824119`.

LC and VdE thank Cristina Cassiago and Enrico Gasparotto, INRIM, for help with a first functionality test of the cryomagnet at the time of purchase.

[1] Bureau International des Poids et Mesures, "SI brochure, 9th edition," 2019. [Online]. Available: https://www.bipm.org/utils/common/pdf/si-brochure/SI-Brochure-9-EN.pdf

[2] R. Ribeiro-Palau, F. Lafont, J. Brun-Picard, D. Kazazis, A. Michon, F. Cheynis, O. Couturaud, C. Consejo, B. Jouault, W. Poirier, and F. Schopfer, "Quantum Hall resistance standard in graphene devices under relaxed experimental conditions," *Nature Nanotech.*, vol. 10, pp. 965–971, 2015.

[3] F. Lüönd, C.-C. Kalmbach, F. Overney, J. Schurr, B. Jeanneret, A. Müller, M. Kruskopf, K. Pierz, and F. Ahlers, "AC quantum Hall effect in epitaxial graphene," *IEEE Trans. Instrum. Meas.*, vol. 66, no. 6, pp. 1459–1466, 2017. [Online]. Available: http://ieeexplore.ieee.org/document/7843592/

[4] M. Kruskopf and R. E. Elmquist, "Epitaxial graphene for quantum resistance metrology," *Metrologia*, vol. 55, no. 4, pp. R27–R36, jul 2018.

[5] A. F. Rigosi, A. R. Panna, S. U. Payagala, M. Kruskopf, M. E. Kraft, G. R. Jones, B. Wu, H. Lee, Y. Yang, J. Hu, D. G. Jarrett, D. B. Newell, and R. E. Elmquist, "Graphene devices for table-top and high-current quantized Hall resistance standards," *IEEE Trans. Instr. Meas.*, vol. 68, no. 6, pp. 1870–1878, June 2019.

[6] F. J. Ahlers, B. Jeanneret, F. Overney, J. Schurr, and B. M. Wood, "Compendium for precise ac measurements of the quantum Hall resistance," *Metrologia*, vol. 46, no. 5, pp. R1–R11, aug 2009.

[7] J. Schurr, F. J. Ahlers, G. Hein, and K. Pierz, "The ac quantum Hall effect as a primary standard of impedance," *Metrologia*, vol. 44, no. 1, pp. 15–23, 2007. [Online]. Available: http://stacks.iop.org/0026-1394/44/i=1/a=002?key=crossref.67449a764062dbba8e9cb9995209f586

[8] J. Schurr, V. Bürkel, and B. P. Kibble, "Realizing the farad from two ac quantum Hall resistances," *Metrologia*, vol. 46, no. 6, pp. 619–628, 2009.

[9] J. Schurr, J. Kučera, K. Pierz, and B. P. Kibble, "The quantum Hall impedance standard," *Metrologia*, vol. 48, no. 1, pp. 47–57, 2011. [Online]. Available: http://stacks.iop.org/0026-1394/48/i=1/a=005?key=crossref.28ed200993947ba3170b8bda9d240e96

[10] L. Callegaro, V. D'Elia, M. Kampik, D. B. Kim, M. Ortolano, and F. Pourdanesh, "Experiences with a two-terminal-pair digital impedance bridge," *IEEE Trans. Instrum. Meas.*, vol. 64, pp. 1460–1465, 2015.

[11] J. Kučera and J. Kováč, "A reconfigurable four terminal-pair digitally assisted and fully digital impedance ratio bridge," *IEEE Trans. Instr. Meas.*, vol. 67, no. 5, pp. 1199–1206, May 2018.

[12] M. Marzano, M. Ortolano, V. D'Elia, A. Müller, and L. Callegaro, "A fully-digital bridge towards the realization of the farad from the quantum Hall effect," submitted.

[13] B. P. Kibble and J. Schurr, "A novel double-shielding technique for ac quantum Hall measurement," *Metrologia*, vol. 45, no. 5, pp. L25–L27, sep 2008.

[14] K. Pierz and B. Schumacher, "Fabrication of quantum Hall devices for low magnetic fields," *IEEE Trans. Instr. Meas.*, vol. 48, no. 2, pp. 293–295, Apr 1999.

[15] F. Delahaye, "Series and parallel connection of multiterminal quantum Hall effect devices," *J. Appl. Phys.*, vol. 73, no. 11, pp. 7914–7920, 1993. [Online]. Available: http://aip.scitation.org/doi/10.1063/1.353944

[16] M. Kruskopf, A. F. Rigosi, A. R. Panna, D. K. Patel, H. Jin, M. Marzano, M. Berilla, D. B. Newell, and R. E. Elmquist, "Two-terminal and multi-terminal designs for next-generation quantized Hall resistance standards: Contact material and geometry," *IEEE Trans. Electron Dev.*, vol. 66, no. 9, pp. 3973–3977, Sep. 2019.